

Estimating stomatal conductance with thermal imagery

I. LEINONEN¹, O. M. GRANT², C. P. P. TAGLIAVIA³, M. M. CHAVES^{2,4} & H. G. JONES¹

¹Division of Environmental and Applied Biology, University of Dundee, Dundee DD2 5DA, Scotland, ²Instituto Tecnologia Química e Biológica, Oeiras, Portugal, ³Department of Biological Sciences, Lancaster University, UK and ⁴Instituto Superior de Agronomia, Lisbon, Portugal

ABSTRACT

Most thermal methods for the study of drought responses in plant leaves are based on the calculation of 'stress indices'. This paper proposes and compares three main extensions of these for the direct estimation of absolute values of stomatal conductance to water vapour (g_s) using infrared thermography (IRT). All methods use the measured leaf temperature and two environmental variables (air temperature and boundary layer resistance) as input. Additional variables required, depending on the method, are the temperatures of wet and dry reference surfaces, net radiation and relative humidity. The methods were compared using measured g_s data from a vineyard in Southern Portugal. The errors in thermal estimates of conductance were of the same order as the measurement errors using a porometer. Observed variability was also compared with theoretical estimates of errors in estimated g_s , determined on the basis of the errors in the input variables (leaf temperature, boundary layer resistance, net radiation) and the partial derivatives of the energy balance equations used for the g_s calculations. The full energy balance approach requires accurate estimates of net radiation absorbed, which may not be readily available in field conditions, so alternatives using reference surfaces are shown to have advantages. A new approach using a dry reference leaf is particularly robust and recommended for those studies where the specific advantages of thermal imagery, including its non-contact nature and its ability to sample large numbers of leaves, are most apparent. Although the results suggest that estimates of the absolute magnitude of g_s are somewhat subjective, depending on the skill of the experimenter at selecting evenly exposed leaves, relative treatment differences in conductance are sensitively detected by different experimenters.

Key-words: *Vitis vinifera*; drought stress; energy balance; infrared thermography; leaf temperature.

INTRODUCTION

Thermal sensing of stomatal closure as an indicator of drought 'stress' has been widely proposed as a plant-based

sensing for irrigation scheduling (see review by Jones 2004), even though most irrigation scheduling is still based on the measurement or calculation of soil moisture deficits. Irrigation scheduling based on sensing of canopy temperature has mostly used stress index approaches (e.g. Idso *et al.* 1981; Jackson *et al.* 1981; Jones 1999; Cohen *et al.* 2005); unfortunately, these generally involve more or less empirical relationships which may only work effectively under specific environmental conditions (see Jones 2004). The fundamental variable sensed by thermal methods is stomatal conductance to water vapour (g_s), but most stress indices are only partly related to conductance, with the index I4 proposed by Jones (1999), being the most closely related. Of wider interest for plant physiologists would be methods that directly estimate g_s from thermal data; possible methodologies have been proposed by various workers using different formulations of the energy balance equations (Jackson *et al.* 1981; Omasa, Hashimoto & Aiga 1981; Smith, Barrs & Fischer 1988; Jones 1999; Kaukoranta *et al.* 2005), although some papers that have reported 'measurement of g_s values' using thermal data have in practice only been reporting relative changes in transpiration (e.g. Prytz, Futsaether & Johnsson 2003).

A general difficulty with thermal methods is that the plant temperature is affected not only by g_s and transpiration, but also by other environmental factors such as air temperature, humidity, radiation and wind speed. Therefore, the estimation of g_s (or plant stress) using temperature measurement requires direct or indirect information about these other factors. One partial solution has been to develop indices that involve the comparison of leaf temperature with appropriate reference temperatures: an important example of this is the crop water stress index (CWSI) (Idso *et al.* 1981; Idso 1982) where the canopy temperature is compared with the temperatures of a notional well-watered crop and a non-transpiring crop. Jones (1999) introduced other indices based on the use of actual wet and dry reference surfaces.

For the widest applicability, rapid methods for estimating actual g_s are required. The main advantages of thermal methods of sensing are that they are more rapid than conventional gas-exchange measurements and do not require physical contact with the leaves, and so do not interfere with the stomatal responses. Infrared thermography (IRT) is a particularly powerful tool, because of its capacity for studying large populations of leaves, so it is possible to

Correspondence: Ilkka Leinonen. Fax: +44 1382 562426; e-mail: i.leinonen@scri.sari.ac.uk

rapidly get information over large areas of canopy (Jones & Leinonen 2003) especially with the use of automated image processing (Leinonen & Jones 2004).

With the increasing application of thermal methods, it is timely to reassess the relative advantages and sensitivities of the various ways in which thermal data can be used to estimate g_s . In this paper, we present three different methods, which are able to directly estimate the absolute g_s using the measurements of leaf temperature, reference surface temperatures and meteorological variables. We demonstrate the applications of these methods using data from a vineyard where the vines were exposed to different irrigation treatments. We also present a detailed evaluation of the potential errors in the g_s estimated by these methods.

MATERIALS AND METHODS

Field experimental data

Experimental data for the comparisons with model calculations were obtained from field measurements of grapevine (*Vitis vinifera* cv. Aragonéz) leaves, performed on 27–28 July 2004 at a commercial vineyard ('Seis Reis') near Estremoz (38°48'N, 7°29'W) in the Alentejo area of South-east Portugal, where the climate is Mediterranean, with hot, dry summers and cool, wet winters. The soils are clay. The vines were grafted on 1103 Paulsen rootstock in 2000 and trained on a bilateral Royal Cordon system. Rows run from 70°E to 250°, with 80 plants per row, and a planting density of 4000 ha⁻¹.

The measurements reported here were primarily from three rows of seven non-irrigated (NI) (no irrigation since 17 June) plants and a similar number of fully irrigated (FI) (100% of the ET_c , half of water supplied to each side of the root system) plants at one end of a larger randomized block irrigation experiment with partial root zone drying (PRD) (50% of ET_c periodically supplied to only one side of the root and sides alternated every 15 d), regulated deficit irrigation (RDI) (% of the ET_c variable over the growing season supplied simultaneously to both sides of the root system) and deficit irrigation (DI) (50% of the ET_c , half of water supplied to each side of the row). The treatments were imposed on 15 June 2004. ET_c was defined according to Allen *et al.* (1999) as the crop evapotranspiration under standard conditions or otherwise known as the 'crop water requirement'. All measurements were taken both on the sunlit and shaded sides of the canopy and utilized a randomized block sampling design.

Thermal images were obtained with two imagers. The first was a SnapShot 525, Infrared Solutions, Minneapolis, MN, USA (supplied by Alpine Components, Oban Road, St. Leonards-on-Sea, East Sussex, UK). This is a 120 × 120 pixel line scan imager that operates in the wavebands 8–12 μm. Any spatial error in temperature estimates was corrected using reference images of the temperature-equilibrated lens cover after every sample image using the method described by Jones *et al.* (2002). Nearly simultaneous digital images were taken to aid the subsequent

analysis of defined leaf or canopy areas in the SnapView Pro (Infrared Solutions) software. The background temperature was determined for each set of measurements as outlined in the manual for the imager. This method entails measuring the temperature of a crumpled sheet of aluminium foil in a similar position to the leaves of interest, with the emissivity set at 1.0. emissivity for measurements of grapevine canopies was set at 0.96. The second imager was a ThermoCAM SC2000 camera (FLIR Systems, West Malling, Kent, UK), which is also a long-wave imager but with a 320 × 240 pixel sensor.

The g_s values of three to five leaves from the canopy area corresponding to each thermal image were measured with an AP4 porometer (Delta-T Devices, Burwell, Cambridge, England) immediately after taking the thermal images. The quoted accuracy of this instrument is ± 20% of conductance reading. Three to five leaves were measured from the canopy area. The meteorological data at 2 m (air temperature, total short-wave radiation, wind speed and relative humidity) were averaged over intervals of 1 min using a Skye MiniMet meteorological station, with an A100R (Vector Instruments, Rhyll, UK) anemometer and an SKS1110/1 pyranometer sensor (Skye Instruments Ltd, Powys, UK). Because the above canopy wind speed overestimated the wind speed, and hence, the boundary layer conductance at the surface of the canopy, the boundary layer conductance was also estimated using heated and unheated leaf models (Brenner & Jarvis 1995). The latter tended to underestimate conductance because they were placed partly inside the canopy to minimize direct solar radiation.

In this study, the net isothermal radiation (R_{ni}) was assumed equal to the absorbed short-wave radiation because preliminary measurements suggested that the other component of R_{ni} , the net long-wave radiation absorbed by the leaf at air temperature (see Jones 1992), is close to zero for vertical leaves at the side of rows. This is because the environment that determines the incoming long-wave radiation on average approximates the leaf temperature for a typical leaf on the vertical side of a vine canopy where the colder sky visible tends to be compensated by the warmer soil. The short-wave solar radiation absorbed by a vertical canopy surface was calculated using Lambert's cosine law from the measured irradiance on a horizontal surface, the orientation of the row and the altitude and azimuth of sun (derived using the equations presented by Jones 1992 and Szokolay 1996). A constant proportion of direct and diffuse radiation and a constant reflectance were assumed, and only the diffuse radiation was included in calculations for the shaded side of the canopy. The diffuse radiation was assumed to be isotropic at 10% of the incoming radiation normal to the solar beam (based on a separate radiation survey carried out within the experimental canopy). For this study, an average value of the boundary layer estimates obtained by the wind speed measurements and by the heated leaves was used to derive a conversion factor for the observed wind speed. In this case, this conversion factor was 0.55. In other situations, different approximations may be more appropriate.

Therefore, for comparison, we also carried out calculations using the original wind speed observations.

Estimation of g_s using leaf temperature measurements

Three basic alternative methods for estimating g_s from leaf temperature measurements with differing requirements for ancillary information are compared; these range from the full energy balance equation [method (a)] to methods that use either dry [method (b)], or dry and wet [method (c)] reference surfaces. The number of ancillary meteorological measurements required depends on the method used. These methods are developed from the basic leaf energy balance (Jones 1992; Jones *et al.* 2002):

$$T_1 - T_a = [r_{HR}(r_{aW} + r_s)\gamma R_{ni} - \rho c_p r_{HR} D] / \{\rho c_p [\gamma(r_{aW} + r_s) + s r_{HR}]\}, \quad (1)$$

where T_1 and T_a (°C) are leaf and air temperatures, respectively, r_s is the leaf resistance to water vapour and assumed to be dominated by the stomatal resistance component ($s \text{ m}^{-1}$), r_{aW} is the boundary layer resistance to water vapour ($s \text{ m}^{-1}$), R_{ni} is the net isothermal radiation [the net radiation for a leaf at air temperature (W m^{-2})], ρ is the density of air (kg m^{-3}), c_p is the specific heat capacity of air ($\text{J kg}^{-1} \text{K}^{-1}$), s is the slope of the curve relating saturating water vapour pressure to temperature ($\text{Pa } ^\circ\text{C}^{-1}$), γ is the psychrometric constant (Pa K^{-1}), r_{HR} is the parallel resistance to heat and radiative transfer ($s \text{ m}^{-1}$) and D is the air vapour pressure deficit (Pa).

(a) Without reference surface temperatures

Stomatal resistance and g_s ($g_s = 1/r_s$) can be directly calculated on the basis of leaf temperature and environmental variables (net isothermal radiation, wind speed, air temperature and relative humidity) by rearrangement of Eqn 1 as:

$$r_s = -\rho c_p r_{HR} [s(T_1 - T_a) + D] / \{\gamma[(T_1 - T_a)\rho c_p - r_{HR} R_{ni}]\} - r_{aW}. \quad (2)$$

This calculation requires not only T_1 , but also measurements of T_a , D , R_{ni} and estimates of r_{HR} and r_{aW} (e.g. from wind speed (u) measurements according to Jones 1992). For T_1 , one leaf at the surface of the canopy (or two or more leaves in the case of SnapShot images) was selected from each thermal image. A circular area was manually extracted from the image and the average temperature of all pixels within this area was calculated.

(b) With dry reference temperature

The need for an estimate of absorbed radiation can be eliminated by using the temperature of a dry reference leaf (T_{dry}). For this one, we can write (Jones 1992):

$$T_{dry} - T_a = R_{ni} r_{HR} / \rho c_p. \quad (3)$$

Assuming that this dry reference has similar aerodynamic (e.g. size, roughness and orientation) and optical (absorbance and exposure to incoming radiation) properties to the

leaf of interest, one can rearrange and substitute for R_{ni} in Eqn 2 to give:

$$r_s = -\rho c_p r_{HR} [s(T_1 - T_a) + D] / [\gamma \rho c_p (T_1 - T_{dry})] - r_{aW}. \quad (4)$$

To estimate T_{dry} , a grapevine leaf, cut from the canopy prior to measurements, was covered in petroleum jelly (Vaseline) on both sides and suspended from a tripod close to the leaves of interest, and with similar orientation and exposure to the measured leaves which were predominantly vertical. The average temperature over a circular area within the dry reference leaf in the thermal image was taken to represent the dry surface temperature. The variables r_{HR} and r_{aW} were estimated according to Jones (1992).

A modification of this approach was also tested (method bi), where all IRT-sensed temperatures, T , were corrected by multiplying by $T_{d,calc}/T_{dry}$, where $T_{d,calc}$ is the temperature of a dry surface as calculated from the environmental measurements (Eqn 3). This directly corrects for any absolute error in the calibration of the infrared sensor because all temperatures are corrected to a common scale [as in method (c)].

(c) With dry and wet reference temperatures

As pointed out by Jones (1999), the requirement for ancillary meteorological data can be further decreased by using the temperatures of both wet (T_{wet}) and dry reference leaves: in this case, the only environmental variables required are the air temperature and the boundary layer resistance allowing stomatal resistance to be directly calculated as:

$$r_s = [r_{aW} + (s/\gamma)r_{HR}](T_1 - T_{wet}) / (T_{dry} - T_1). \quad (5)$$

However, the above equation is valid only in the case that the boundary layer resistance to water vapour is equal for the plant leaf and reference leaves. For hypostomatous leaves used together with reference leaves for which both sides are wet, one should substitute the appropriate different values for r_{aW} in the derivation presented by Jones (1999) to give the following:

$$r_s = [0.92 r_{aH} + (s/\gamma)r_{HR}](T_{dry} - T_{wet}) / (T_{dry} - T_1) - 1.84 r_{aH} - (s/\gamma)r_{HR}, \quad (6)$$

where $0.92 r_{aH}$ and $1.84 r_{aH}$ indicate the boundary layer resistance to water (r_{aW}) for wet reference leaves and for hypostomatous plant leaves, respectively. T_{wet} was measured on another grapevine leaf cut from the canopy prior to measurements and mounted adjacent to the dry reference leaf, but maintained wet by regular spraying on both sides with water and detergent.

In the few cases where physically unrealistic conductances (> 1200 or $< 0 \text{ mmol m}^{-2} \text{ s}^{-1}$) were calculated, for the statistical analyses, values were set, respectively, as 1200 or $0 \text{ mmol m}^{-2} \text{ s}^{-1}$ as the nearest physically realistic values.

Uncertainty analysis

The uncertainty in estimates of g_s (σ_{g_s}) can be calculated on

the basis of the errors in measurement of the input variables. Errors in the following variables need to be considered: boundary layer resistance (affected by wind speed and the leaf dimensions and orientation), radiation, humidity, air temperature and leaf temperature (or leaf – air temperature difference). In addition, the reference leaf methods will also be subject to errors in estimates of the reference temperatures. These errors include: (1) random errors arising from both instrument noise and temporal lags between measured values and the relevant responses (e.g. as a result of spatial separation of anemometer or radiometer and the leaf of interest); and (2) bias errors resulting from miscalibration of sensors or erroneous conversion factors. Random and bias errors are considered separately as they have different impacts on the analysis.

One way to estimate the uncertainty is the use of simulation methods such as the Monte Carlo approach. However, for practical purposes, an analytical method is valuable for estimating the potential error of the g_s estimates in various environmental conditions. Unfortunately, precise calculation of the random errors is difficult because of the complexity of Eqns 2, 4 and 6, the fact that some variables show a measure of covariance, and the fact that various ‘constants’ involved all have different temperature sensitivities. Therefore, we developed a simplified analytical method for error propagation considering the most important variables that are potential sources of uncertainty as derived from the preliminary analysis. These variables are leaf temperature, reference temperatures, radiation and boundary layer resistance (estimated from wind speed measurements and/or heated leaves). Although air temperature affects several variables, these effects can usually be considered to be minor, and are excluded from the analytical error analysis in this study. Furthermore, based on simulation tests, small errors in the measurements of relative humidity were found to have only a minor effect on the estimated g_s , while any effects of varying leaf orientation with respect to the airflow can be incorporated in the wind speed error. Details of the random error calculations may be found in the Supplementary Material available online (Fig. S1).

In the analytical method, the uncertainty of the output variable (r_s) is calculated by multiplying the errors in the input variables by the partial derivatives of the function r_s with respect to the input variable. For comparison, the analytical results were compared with a Monte Carlo approach where a normally distributed random error (obtained using the NORMINV function in Excel and applying an appropriate SD) was superimposed on each of the measured variables. This method also incorporated the full effect of errors in air temperature measurements and the errors in the humidity measurements, which were excluded from the analytical approach. Three thousand simulations were run for each set of environmental conditions or error magnitudes.

The sensitivity of estimates of r_s to bias in temperature measurements was estimated by partial differentiation of the appropriate Eqns 2, 4 or 6 with respect to the leaf–air temperature difference and substitution of typical values of

the various variables. Details of the relevant partial derivatives may be found in the Supplementary Material available online (Fig. S1).

Errors in input variables

The specification of thermal imagers varies substantially. The ThermaCAM SC2000 has a quoted noise equivalent temperature difference (NETD) of $< 0.08\text{K}$, and an accuracy of $\pm 2\text{K}$ or 2%, which are typical of portable uncooled thermal imagers, and the SnapShot 525 has an NETD of $< 0.4\text{K}$ and an accuracy of $\pm 2\text{K}$. The NETD is calculated on a single pixel basis; averaging over larger numbers of images or pixels can improve the effective sensitivity. The SD of the temperatures of individual pixels over the central areas of selected homogeneous leaves averaged $0.23\text{ }^\circ\text{C}$ for the Snapshot and $< 0.1\text{ }^\circ\text{C}$ for the ThermaCAM over a number of studies in different environments. In a number of individual tests in a range of environments, the absolute leaf temperatures recorded for both cameras were within $1\text{ }^\circ\text{C}$ of the values obtained using fine-wire copper–constantan thermocouples and usually within $0.4\text{ }^\circ\text{C}$. These values correspond with or exceed the specifications of the two instruments. For the uncertainty analysis of the field data in this study, we used the value of $1\text{ }^\circ\text{C}$ as a very conservative estimate for the random error of both leaf and reference temperature measurements.

The anemometer used has a quoted accuracy of 1% of wind speed. However, in the field measurements of this study, the estimate of wind speed used in the model calculations was an average of two very different measurements, both separating spatially from the location of the leaf temperature measurements. Therefore, wind speed was probably the most uncertain of all measured variables, and we used a relative error as high as 50% in the uncertainty analysis. The humidity sensors had an accuracy of better than 2%.

The quoted typical uncertainty for the pyranometer sensor is $\pm 3\%$ of the reading, to which must be added the uncertainty that arises from the spatial separation of leaf and sensor and the uncertainty that arises from variation in leaf angle. In the present study, leaves were selected for analysis with orientations differing by no more than about ± 5 which equates to $< 1\%$ random error in radiation received by leaves nominally normally oriented to the beam increasing to *c.* 10% for leaves at 45° and even more as the angles become more acute. Further bias may arise from our assumption that R_{in} equates to R_s (the absorbed short-wave irradiance). In addition, there may be some direct radiation coming through the canopy (against our assumption) at the shaded side of the row. For these reasons, a constant error, the magnitude of which was 20% of the maximum measured radiation value of each data set, was used for the uncertainty analysis of the field data.

Statistical analysis

Statistical analysis was performed using Minitab 13.1 (State

College, PA, USA). For analyses of variance (ANOVAs), Bartlett's test was used to test for the homogeneity of variance, in no case was the slight tendency for the variance of conductance to increase with the mean strong enough to justify data transformation. Leaf-to-leaf variation (cv_{leaf}) was estimated as the square root of the error mean square from an ANOVA (i.e. after eliminating block and treatment effects) and dividing by the mean to give the coefficient of variation.

RESULTS

Field measurements

An initial replicated survey of the experiment with paired measurements where each camera imaged a similar area of canopy within about 30 s allowed a comparison of the two cameras. For 24 pairs of near-simultaneous images, the mean canopy temperatures recorded by the two cameras were within $0.2\text{ }^{\circ}\text{C}$ (using the corrected SnapShot values). The image-image SDs (s_{image}) of comparable canopy areas (from the error mean square of an ANOVA after removing all treatment and block effects) was $1.64\text{ }^{\circ}\text{C}$ for the ThermaCAM and $2.25\text{ }^{\circ}\text{C}$ for the SnapShot. These values include both instrument error and, much more importantly, both 'operator' errors in identifying comparable areas of canopy and short-term variation in true canopy temperature. Nevertheless, the correlations between temperatures obtained with the two cameras were high, with the correlation coefficient between ThermaCAM and SnapShot readings equalling 0.94, or higher depending on the experiment.

Sample relationships between reference surface temperatures measured with the ThermaCAM and the corresponding temperatures calculated using environmental measurements are shown in Fig. 1. In general, the relationship was close, although with a clear indication that the calculated temperatures for any treatment were more stable than the observed temperatures and did not fully reflect the short-term local variability; for the wet reference, part of the variability arises because of the difficulty of maintaining a leaf fully wetted (Grant *et al.*, unpublished results). The high covariance between the temperatures of both references and the leaves (r usually > 0.75) indicates that much of the short-term variability would be accounted for in methods using reference temperatures. It is also worth noting that there was a tendency, especially with the late evening measurements (b), for the calculated temperatures to overestimate the reference temperatures, possibly as a result of the model overestimating the actual radiation received at these solar elevations.

On each measurement occasion, the g_s values were measured on 3–5 individual leaves per plot from the area included in each of the thermal images. Some typical comparisons between the calculated (thermal) and measured (porometer) conductances are shown in Fig. 2. These illustrate the differences between the various thermal calculation methods and between independent temperature estimates (made by different researchers) on the same

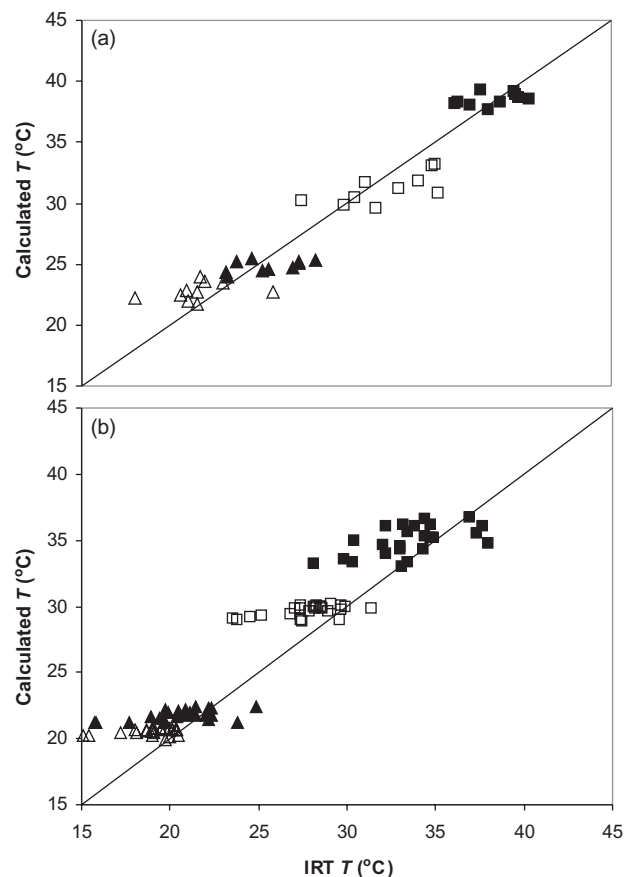


Figure 1. Relationship between calculated and observed (ThermaCAM) temperatures of wet (\blacktriangle) and dry (\blacksquare) reference leaves. Filled symbols are for the sunlit side of the canopy and open symbols are for the shaded side. (a) Measurements between 1050 and 1240 h on 27 July 2004. (b) Measurements taken between 1700 and 1805 h on 28 July 2004. IRT, infrared thermography.

thermal images. Table 1 summarizes some typical treatment means together with leaf-leaf variation (cv_{leaf}) for each method/data set. This 'leaf-leaf' variation incorporates instrumental error, temporal changes, leaf-to-leaf and within-leaf variation: unfortunately, it is not easy reliably to separate these sources of error. The coefficient of variation for the porometer measurements of conductance was around 30%, but increased to between 32 and 46% for most of the thermal estimates. Nevertheless, in most cases, the treatment effects showed similar significance levels for porometer and thermal estimates. The accuracy of different methods varied between the data sets. Across a range of studies, the use of a dry reference with all imager temperatures corrected according to the calculated dry reference (method bi) was the most consistent and closest to the porometer measurements, while method (a) tended to be least accurate.

The results (Table 1; Fig. 2) illustrate the fact that in many cases, the different calculation methods tend to overestimate g_s compared with the porometer measurements especially in the case of the 28 July data set. The degree of

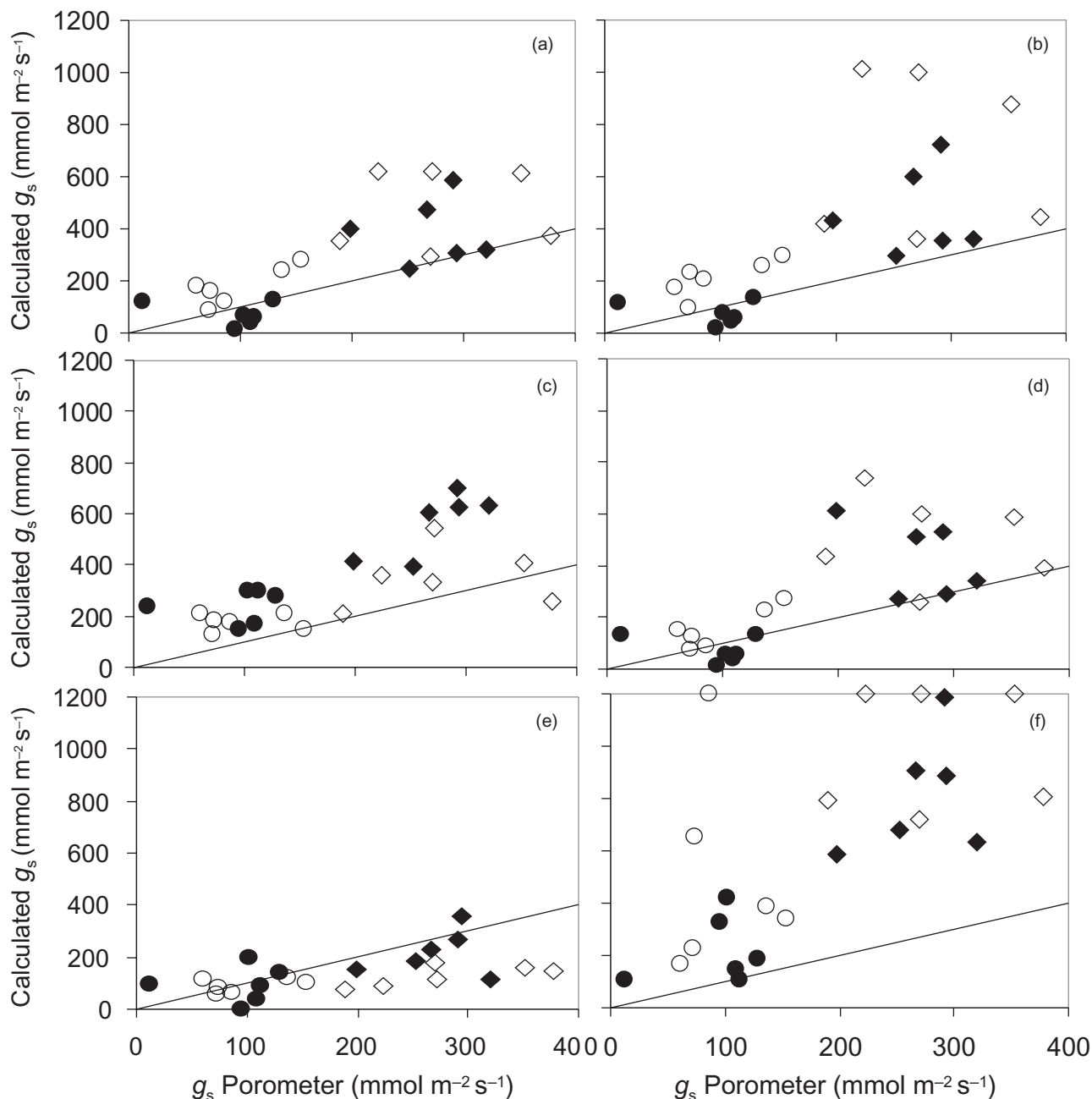


Figure 2. The relationship between calculated and measured stomatal conductances to water vapour (g_s) for data from 28 July 2004. Each point is the mean of data for each block/treatment combination. (a, b, d & f) For one assessor identifying single leaves. (c) For the same user identifying a larger area from the image. (e) For an independent analyst. The methods applied are bi (a, c & e); b (b); c (d); and a (f). The open symbols are for data on the shaded canopy and the closed symbols for the sunlit canopy, while fully irrigated (FI) treatment (diamonds) and non-irrigated (NI) treatment (circles) are indicated. The 1:1 line is shown.

overestimation, however, is dependent on the subjective selection of leaves by the analyst, as can be seen from a comparison of the 28 July data (e.g. compare Fig. 2a & c), with the latter apparently selecting a different subset of leaves. The overestimation may also be caused by systematic errors in the measurements of the environmental data, and also by the fact that the relationship between leaf temperature and g_s is non-linear. This means that underestimation of leaf temperature causes higher error (overestimate)

in calculated g_s than similar overestimation of leaf temperature. Only in a few cases did the underestimation of the leaf temperature cause any unrealistic estimates of g_s ($g_s > 1200 \text{ mmol m}^{-2} \text{ s}^{-1}$), although in one case the proportion reached 22% when method (a) was used.

In spite of the differences in absolute value, there were consistent correlations (expressed as R^2 or the percentage of variance explained) between the calculated conductances and the porometer measurements of g_s ; these values

Table 1. Samples of the different estimates of treatment means of stomatal conductance to water vapour (g_s) ($\text{mmol m}^{-2} \text{s}^{-1}$) for SnapShot measurements on 27 July 2004 (1055–1240 h; $n = 48$) and ThermoCAM measurements on 28 July 2004 (1650–1800 h; $n = 48$), as compared with porometer estimates.

(mmol m ⁻² s ⁻¹)	27			28			28			28			28		
	Leaf 1 (a)	Leaf 1 (b)	Leaf 1 (c)	Leaf 1 (bi)	Porometer	Leaf 2 (a)	Leaf 2 (b)	Leaf 2 (c)	Leaf 2 (bi)	Leaf 2 (a)	Leaf 2 (b)	Leaf 2 (c)	Leaf 3 (a)	Leaf 3 (bi)	Area 4 (bi)
FI – sun	503	678	855	751	270	814	461	428	390	485	218	485	485	218	564
FI – shade	469	313	191	271	281	986	685	501	480	416	128	416	416	128	352
NI – sun	364	319	323	303	94	216	76	72	72	250	94	250	250	94	240
NI – shade	70	146	131	168	98	495	211	157	179	396	90	396	396	90	177
Mean	352	364	375	373	185	628	358	289	280	387	133	387	387	133	333
cv_{leaf}	0.37	0.46	0.40	0.38	0.30	0.41	0.42	0.32	0.38	0.57	0.47	0.57	0.57	0.47	0.50
Irrigation P	0.103	0.012	0.003	0.012	< 0.000	< 0.000	< 0.000	< 0.000	< 0.000	0.281	< 0.000	0.281	0.281	< 0.000	< 0.000
Shading P	0.303	0.011	< 0.000	0.016	0.017	0.046	0.024	< 0.000	0.037	0.744	0.013	0.744	0.744	0.013	0.002
R^2	0.514	0.739	0.719	0.715		0.673	0.691	0.710	0.759	0.204	0.556	0.204	0.204	0.556	0.704

Data are shown for four different calculation methods (a, b, bi and c) and independent temperature estimates from the images (leaf 1, leaf 2, leaf 3 and area 4) are compared. The leaf–leaf variation (cv_{leaf}) is estimated for each method and the probability levels (P) for irrigation and shading comparisons are shown, together with the R^2 between the porometer readings and each thermal conductance estimate.

FI, fully irrigated; NI, non-irrigated.

are close to what would be expected for similar error magnitudes for the two variables. As an approximate test of this statement for the 28 July data, we took the observed plot mean conductances and simulated (using the NORMINV function in Excel) the component individual conductances using the plot means and the observed overall g_{leaf} of 56.2, and then simulated the calculated conductance using the same error. Over 40 simulations R^2 averaged 0.594, which is actually lower than most of the observed values.

Summarizing the results from a large series of analyses showed that although the magnitude of the error is rather little affected by the operator or area selected, the absolute values appear to be rather subjective depending on the leaf selection for analysis. The close fit (e.g. Fig. 2e) occurs where the operator selected well-exposed leaves, while the area image (Fig. 2c) is biased to lower temperatures, and therefore, higher conductances (at least on the sunlit side of the canopy) as it included some shaded (and hence, cooler) areas than the relevant reference surfaces.

Model calculations of potential errors

In addition to the direct observations based on the field data, the uncertainty in g_s estimates using the four IRT methods was analysed using theoretical calculations. In these calculations, the environmental conditions were set constant and similar to the values for the field experiment. Figure 3 shows, for two representative data sets, the magnitude of the uncertainty for individual IRT estimates in comparison with the observed SD of porometer estimates. It is notable, that even though the rather large values for the errors of the leaf temperature and wind speed measurements were used, the magnitude of the error in the g_s estimates was rather similar for IRT calculations and porometer estimates, with the porometer values (horizontal bars) tending to be the larger. This result indicates that although the accurate estimation of the level of wind speed at the canopy surface may be difficult in field conditions, the error is not necessarily critical. For example, if the original wind speed value was used instead of the corrected value, the difference in the g_s estimates was only about 20%, on average, when the method with the dry reference leaf was used (results not shown).

The dependence of the uncertainty in the estimates of g_s on g_s and on environmental variables was either simulated using the Monte Carlo approach or by the analytical method. In this analysis, the magnitude of the input errors was set smaller than in the field data of this study, assuming that the conditions of the measurements of environmental variables are optimal and that the input error is mainly limited to the instrumental error. Figure 4 shows how the magnitude of the random error in estimates of g_s , as calculated using the analytical method, varies as environmental conditions and g_s change over a likely range of environmental conditions. For each environmental factor, the left-hand graphs indicate the absolute error and the right-hand graphs indicate the relative error in g_s . In general, although the absolute error decreases monotonically as the leaf

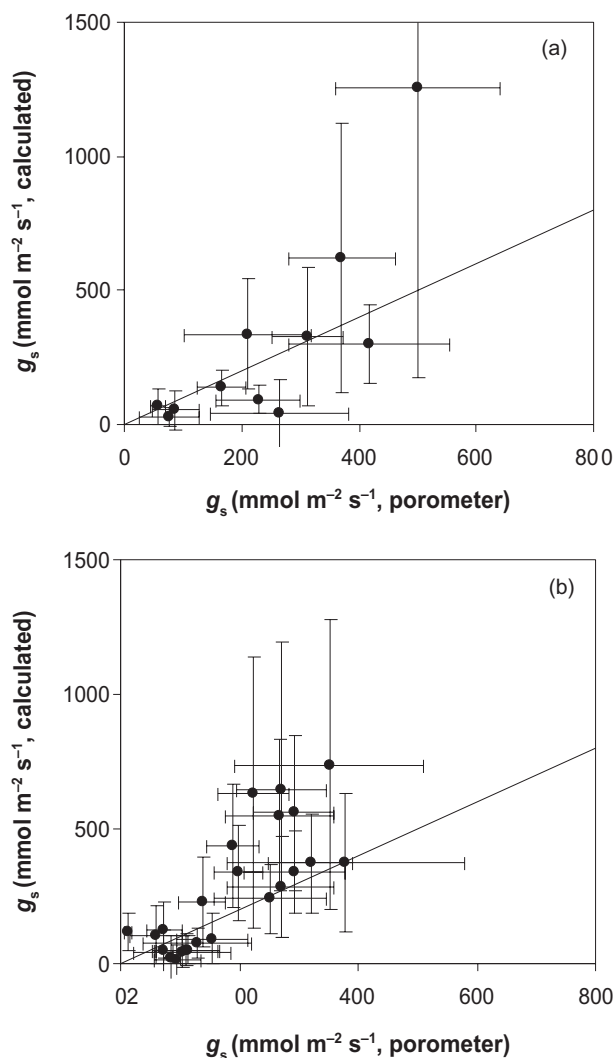


Figure 3. Examples showing the calculated uncertainty (σ_{gs}) of individual conductance estimates (with error bars calculated using the analytical method) and stomatal conductance to water vapour (g_s) measured with porometer (with SD). (a) Data for 27 July [method (b)]. (b) Data for 28 July [method (c)]. The diagonal line indicates 1:1 relationship between the measured and calculated g_s .

conductance decreases, the relative error in estimates of g_s can increase substantially as g_s decreases below 100–200 $\text{mmol m}^{-2} \text{s}^{-1}$. The uncertainty for methods (b) and (c) (and bi – not shown) was generally very similar and less than the corresponding value for method (a) (Fig. 4). The magnitude of the error increases as air humidity increases, and when the temperature differences between wet and dry leaves decrease. The error also increases as the air temperature decreases, although the sensitivity to radiation depends strongly on the method used (Fig. 4c & d). The response to wind speed is also complex: at low g_s values the error increases with wind speed, but at high conductances the error decreases with increasing wind speed.

The magnitudes of uncertainties obtained using the analytical and Monte Carlo methods were rather similar,

although with a tendency for the Monte Carlo simulations to give slightly larger errors (detailed results not shown). It is also notable that the Monte Carlo simulation generally predicted higher mean g_s values (usually by < 2%, but reaching 5% for g_s of 800 $\text{mmol m}^{-2} \text{s}^{-1}$ and $\sigma_T = 0.4\text{K}$) than those calculated using the means of all input variables (Eqns 2, 4 & 6). Larger errors and overestimated absolute values of g_s in the Monte Carlo method arise from the non-linearities in the responses so that the mean effect of a normally distributed error in a component variable can lead to a bias in the result.

The sensitivity of the overall uncertainty to random errors in individual environmental measurements is investigated in Table 2. It is clear from this that the most critical measurements are of leaf (and reference surface) temperatures, and for method (a), of net radiation. Even quite large uncertainties in wind speed or T_a measurement have relatively small effects on the error in the estimate of g_s . Note that absolute leaf temperatures only need to be known accurately for methods (a) and (b). The uncertainty arising from errors in infrared measurements of temperatures is much greater for the models using reference surfaces than for model (a) where only leaf temperatures are used. Interestingly, the errors are similar for both methods (b) and (c), even though the latter has an extra temperature measurement. This is because of the fact that the errors in terms $T_{\text{dry}} - T_{\text{wet}}$ and $T_{\text{dry}} - T_1$ partly offset each other.

Systematic errors in infrared temperature estimates have an effect on the estimated g_s only when the method without reference leaves (a) or the method with the dry reference leaf alone (b) is used. The relative magnitude of this error is simply the partial derivative of the equation for r_s with respect to variable $T_1 - T_a$, divided by the calculated value of stomatal resistance. An example of the dependence of the relative systematic errors in g_s as a result of systematic temperature error is shown in Fig. 5.

DISCUSSION

IRT or thermometry for estimating g_s has a number of advantages in comparison with conventional porometry.

Table 2. Dependence of the magnitude of the uncertainty in estimates of stomatal conductance to water vapour (g_s) on the magnitude of the component errors, expressed as a percentage increase in uncertainty of g_s in response to a doubling (independently) of each component error

Error (%)	T	R_{ni}	T_a	u
(a) No reference surface	38	82	11	7
(b) Dry reference	95	n.a.	1	12
(c) Wet and dry reference	97	n.a.	1	21

All values expressed relative to the uncertainty of estimate at $g_s = 200 \text{ mmol m}^{-2} \text{s}^{-1}$ under the following error assumptions: $\sigma_u = 5\%$, $\sigma_{R_{\text{ni}}} = 5\%$, $\sigma_T = 0.2 \text{ }^\circ\text{C}$ (all temperature measurements). R_{ni} , net isothermal radiation; T_a , air temperature; u , wind speed; n.a., not applicable.

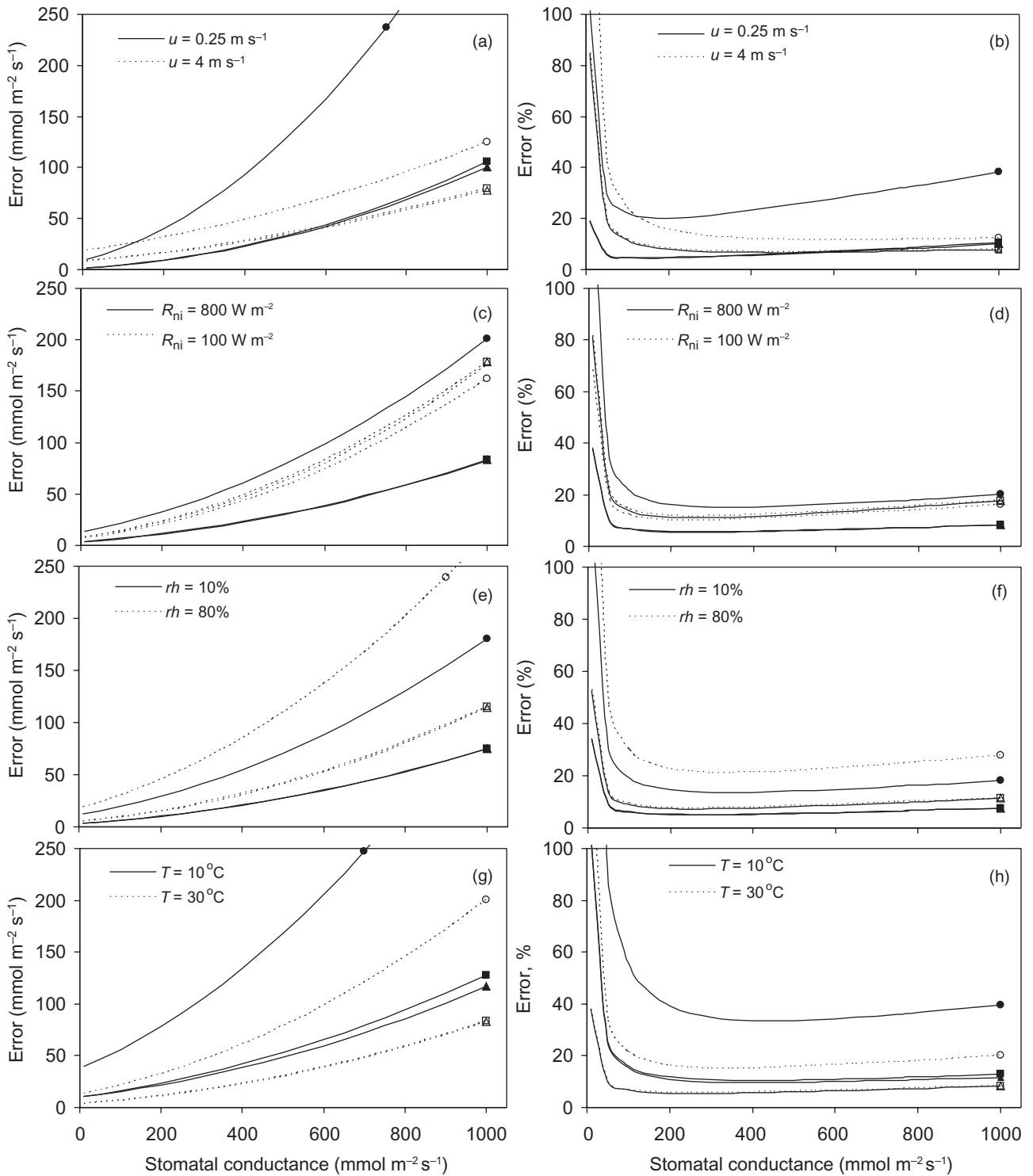


Figure 4. Variation in absolute (a, c, e & g) and relative (b, d, f & h) error in estimates of stomatal conductance to water vapour (g_s) for varying environmental conditions: wind speed (a, b); net radiation (c, d); relative humidity (e, f); and air temperature (g, h). The standard conditions assumed were $T_a = 30\text{ }^\circ\text{C}$, $R_{ni} = 800\text{ W m}^{-2}$, $u = 1\text{ m s}^{-1}$, $rh = 30\%$. Input errors were $0.2\text{ }^\circ\text{C}$ for leaf and reference temperatures and 5% for R , u and rh . Circles, method (a), no reference leaves; squares, method (b), dry reference leaf; triangles, method (c), dry and wet reference leaves.

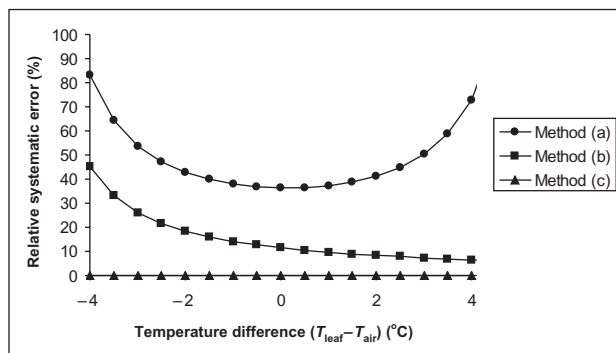


Figure 5. The relative systematic error of stomatal resistance as a result of 1 °C bias in leaf and reference temperature measurements. Environmental conditions: $T_a = 30$ °C, $R_{ni} = 360$ W m⁻², $rh = 30\%$.

Most importantly, thermal methods require no physical contact with leaves and therefore do not disturb the stomatal functioning. Thermal methods also allow a continuous recording of stomatal behaviour for large numbers of leaves without the need to enclose the leaves in measurement chambers. Previously available thermal sensing methods (see Jones 2004) only allowed an estimation of relative changes in g_s ; the methods presented here now provide absolute estimates of conductance, as required in many physiological studies. Imaging is also much faster, allows much greater replication and therefore is potentially less labour intensive than porometry. As large canopy areas can be observed at the same time, canopy averages are more readily obtained. As the present results show, thermal methods can estimate the differences in g_s , for example, between different irrigation treatments, equally or even more accurately than porometer measurements.

Notwithstanding the advantages of thermal sensing, each of the methods available has limitations, which should be taken into account when selecting either porometry-based or thermal-based methods. Based on the experimental results of this study and on the theoretical error analyses, the usefulness of different methods in different conditions can be evaluated. In general, all thermal methods require additional environmental variables for estimation of g_s . The need for meteorological measurements may seem to limit the usefulness of thermal imaging in field conditions. Despite this, the possibility for automating the environmental observations and calculations makes the use of thermal methods very practical in many situations. Most of the environmental variables can be obtained using standard meteorological measurements. Estimating the wind speed at the canopy surface may be in some cases difficult because a specific correction factor is required. However, the results show that correct wind speed estimates are not very critical in estimation of g_s . This can be explained by the fact that the relationship between wind speed and boundary layer resistance is non-linear, and even a large variation of the wind speed under typical field conditions has little effect.

In this study, three main approaches to using leaf temperature measurements for estimating g_s are proposed and evaluated. A method that uses both dry and wet reference temperatures has been previously applied in field conditions for estimating a stress index related to g_s (Jones 1999; Jones *et al.* 2002). In the present study, this method is extended to calculate the absolute g_s directly, incorporating also a modification to take account of the differences of the boundary layer conductance to water vapour for hypostomatous plant leaves and wet reference leaves. The other methods use either only a dry reference or no references, where all the necessary ancillary information is obtained from meteorological instruments.

Method (a), utilizing the full energy balance of a leaf, requires only the temperature of the plant leaf in addition to environmental data. The main problem of this method is to obtain an accurate estimate of the net radiation absorbed by the leaf. In practice, the radiation is usually measured at a single point differing spatially from the canopy area of interest. Therefore, certain corrections based on simplified assumptions should be done for the measured radiation values. This requirement, together with the need for the absolute leaf temperature to be measured accurately, limits the wide application of this method. Indeed, both the experimental data and the theoretical calculations show that this method has usually the highest error and the lowest prediction power of all the compared thermal methods. These errors can be reduced substantially, however, by undertaking measurements only on the shaded side of the canopy, where variation of radiation is a smaller component of the energy balance (Jones *et al.* 2002).

The use of reference surfaces eliminates the requirement for high absolute accuracy with the leaf temperature measurements and also eliminates the need for radiation measurements. Although the use of wet and dry surfaces together eliminates the need for humidity measurements, humidity is easily measured with reasonable precision. In practice, it is much more difficult to maintain a reference leaf wet than it is to maintain a dry reference, so we recommend that the most practical approach is that based on the use of a dry reference [method (b)]. Although the results show that the accuracy of g_s estimates is even higher when using a modification with empirically corrected leaf temperatures (method bi), this method does require measurements of radiation [not required for method (b)]. A slight disadvantage of method bi is that the uncertainty of the calculated g_s cannot readily be estimated analytically.

As a conclusion, we suggest that methods using IRT or thermometry have significant advantages in estimating plant g_s compared to traditional porometry. This is especially the case in long-term monitoring of crop water status because of reduced requirements of labour. For most applications, we recommend the method utilizing the measurements of dry reference surface temperature. In cases where maintaining the reference surfaces is difficult, the method based on the full leaf energy balance can be used, although it may give less accurate estimates of g_s .

ACKNOWLEDGMENTS

This work was funded through the EC Research Training Network STRESSIMAGING (HPRN-CT-2002-00254) with some additional input from Defra HortLINK project HL0168. We thank Lukasz Tronina and Solja Lipitsäinen for assistance in field measurements.

REFERENCES

- Allen R.G., Pereria L.S., Raes D. & Smith M. (1999) *Crop Evapotranspiration: Guidelines for Computing Crop Water Requirements*. FAO 56. FAO Land and Water Division, Rome, Italy.
- Brenner A.J. & Jarvis P.G. (1995) A heated leaf replica technique for determination of leaf boundary layer conductance in the field. *Agricultural and Forest Meteorology* **72**, 261–275.
- Cohen Y., Alchanatis V., Meron M., Saranga Y. & Tsipris J. (2005) Estimation of leaf water potential by thermal imagery and spatial analysis. *Journal of Experimental Botany* **56**, 1843–1852.
- Idso S.B. (1982) Non-water-stressed baselines: a key to measuring and interpreting plant water stress. *Agricultural Meteorology* **27**, 59–70.
- Idso S.B., Jackson R.D., Pinter P.J., Reginato R.J. & Hatfield J.L. (1981) Normalizing the stress–degree–day parameter for environmental variability. *Agricultural Meteorology* **24**, 45–55.
- Jackson R.D., Idso S.B., Reginato R.J. & Pinter P.J. (1981) Canopy temperature as a crop water-stress indicator. *Water Resources Research* **17**, 1133–1138.
- Jones H.G. (1992) *Plants and Microclimate*, 2nd edn. Cambridge University Press, Cambridge, USA.
- Jones H.G. (1999) Use of infrared thermometry for estimation of stomatal conductance as a possible aid to irrigation scheduling. *Agricultural and Forest Meteorology* **95**, 139–149.
- Jones H.G. (2004) Application of thermal imaging and infrared sensing in plant physiology and ecophysiology. *Advances in Botanical Research* **41**, 107–163.
- Jones H.G. & Leinonen I. (2003) Thermal imaging for the study of plant water relations. *Journal of Agricultural Meteorology* **59**, 205–217.
- Jones H.G., Stoll M., Santos T., de Sousa C., Chaves M.M. & Grant O.M. (2002) Use of infrared thermography for monitoring stomatal closure in the field: application to grapevine. *Journal of Experimental Botany* **53**, 2249–2260.
- Kaukoranta T., Murto J., Takala J. & Tahvonen R. (2005) Detection of water deficit in greenhouse cucumber by infrared thermography and reference surfaces. *Scientia Horticulturae* **106**, 447–463.
- Leinonen I. & Jones H.G. (2004) Combining thermal and visible imagery for estimating canopy temperature and identifying plant stress. *Journal of Experimental Botany* **55**, 1423–1431.
- Omasa K., Hashimoto Y. & Aiga I. (1981) A quantitative analysis of the relationships between O₃ sorption and its acute effects on plant leaves using image instrumentation. *Environmental Control in Biology* **19**, 85–92.
- Prytz G., Futsaether C.M. & Johnsson A. (2003) Thermography studies of the spatial and temporal variability in stomatal conductance of *Avena* leaves during stable and oscillatory transpiration. *New Phytologist* **158**, 249–258.
- Smith R.C.G., Barrs H.D. & Fischer R.A. (1988) Inferring stomatal resistance of sparse crops from infrared measurements of foliage temperature. *Agricultural and Forest Meteorology* **42**, 183–201.
- Szokolay S.V. (1996) *Solar Geometry. Passive and Low Energy Architecture*. Note 1. University of Queensland, Brisbane, Australia.

Received 3 March 2006; received in revised form 7 March 2006; accepted for publication 8 March 2006

SUPPLEMENTARY MATERIAL

The following supplementary material is available for this article online:

Figure S1. Details of the random error calculations and of the relevant partial derivatives.

This material is available as part of the online article from <http://www.blackwell-synergy.com>